J|A|C|S
ARTICLES
Published on Web 04/20/2002

Mapping the Cytochrome *c* Folding Landscape

Julia G. Lyubovitsky, Harry B. Gray,* and Jay R. Winkler*

Contribution from the Beckman Institute, California Institute of Technology, Pasadena, California 91125

Received October 26, 2001

Abstract: The solution to the riddle of how a protein folds is encoded in the conformational energy landscape for the constituent polypeptide. Employing fluorescence energy transfer kinetics, we have mapped the *S. cerevisiae* iso-1 cytochrome *c* landscape by monitoring the distance between a C-terminal fluorophore and the heme during folding. Within 1 ms after denaturant dilution to native conditions, unfolded protein molecules have evolved into two distinct and rapidly equilibrating populations: a collection of collapsed structures with an average fluorophore−heme distance ($\bar{r}$) of 27 Å and a roughly equal population of extended polypeptides with $\bar{r} > 50$ Å. Molecules with the native fold appear on a time scale regulated by heme ligation events (~300 ms, pH 7). The experimentally derived landscape for folding has a narrow central funnel with a flat upper rim on which collapsed and extended polypeptides interchange rapidly in a search for the native structure.

Introduction

The production of functional proteins requires that polypeptides find a unique conformation in a vast space of incorrect folds.[1] The consequences of failure are severe; misfolded proteins are implicated in a rapidly growing list of debilitating illnesses that includes type II diabetes as well as Alzheimer's and Creutzfeldt−Jakob diseases.[2] Partially folded polypeptide structures are key intermediates in both the proper assembly of proteins and the formation of harmful misfolded structures.[3−5] Characterizing the structures, energetics, and dynamics of these transient species is an essential step in understanding their benign and malignant pathways.

Proteins often fold quite rapidly (<1 s), because the energy bias on a funnel-shaped landscape steers unfolded peptides toward native conformations.[6,7] The upper rim of the funnel represents a heterogeneous ensemble of unfolded polypeptides; partially folded conformations appear as local minima on this energy surface; and misfolded structures can be in deep energy wells separate from the native minimum. To map this complex energy landscape, it is necessary to probe structural features of the polypeptide ensemble as it evolves to the native state.

The distribution of distances between donor (**D**) and acceptor (**A**) labeled residues in a polypeptide can be extracted from an analysis of fluorescence energy transfer (FET) kinetics.[8] An ensemble of unfolded polypeptides should have a broad **D**−**A** distribution ($P(r)$) (Figure 1), with a mean value ($\bar{r}$) that increases with the number of residues between **D** and **A**. The many different distances in this ensemble produce a distribution of fluorescence decay rates ($P(k)$) and a highly nonexponential decay profile ($I(t)$) (Figure 1). By contrast, a folded protein will have a narrow $P(r)$ range, a smaller value of $\bar{r}$, and faster, albeit still nonexponential decays.

We have examined **D**−**A** distance distributions during the folding of *Saccharomyces cerevisiae* iso-1 cytochrome *c* (cyt *c*), a 108-residue, partially helical, heme protein.[9] In prior work, we have shown that the folding kinetics (corrected for driving force) of iso-1 cyt *c* are comparable to those of the more extensively studied equine protein.[10−15] In the folded protein at neutral pH, an imidazole nitrogen (H18)[16] and a thioether sulfur (M80) axially ligate the heme iron. The nitrogenous base of an amino acid side chain (pH 7: H26, H33, H39) replaces M80 in the unfolded protein.[17] This misligation retards refolding, because ligand exchange is required for the peptide to adopt its native conformation.[18,19] For FET kinetics experiments, we derivatized the thiolate sulfur of C102 in yeast cytochrome *c*

* Corresponding author. E-mail: winklerj@caltech.edu.

(1) Dill, K. A.; Chan, H. S. *Nature Struct. Biol.* **1997**, *4*, 10−19.
(2) Dobson, C. M. *Philos. Trans. R. Soc. B* **2001**, *356*, 133−145.
(3) King, J.; Haase-Pettingell, C.; Robinson, A. S.; Speed, M.; Mitraki, A. *FASEB* **1996**, *10*, 57−66.
(4) Nielson, L.; Ritu, K.; Coats, A.; Frokjaer, S.; Brange, J.; Vyas, S.; Uversky, V. N.; Fink, A. L. *Biochemistry* **2001**, *40*, 6036−6046.
(5) Chiti, F.; Webster, P.; Taddei, N.; Clark, A.; Stefani, M.; Ramponi, G.; Dobson, C. M. *Proc. Natl. Acad. Sci. U.S.A.* **1999**, *96*, 3590−3594.
(6) Bryngelson, J. D.; Onuchic, J. N.; Wolynes, P. G. *Proteins*: *Struct. Func. Gen.* **1995**, *21*, 167−195.
(7) Onuchic, J. N.; Lutheyschulten, Z.; Wolynes, P. G. *Annu. Rev. Phys. Chem.* **1997**, *48*, 545−600.
(8) Navon, A.; Ittah, V.; Landsman, P.; Scheraga, H. A.; Haas, E. *Biochemistry* **2001**, *40*, 105−118.
(9) Scott, R. A.; Mauk, A. G. *Cytochrome c−A Multidisciplinary Approach*; University Science Books: Sausalito, CA, 1996.
(10) Mines, G. A.; Pascher, T.; Lee, S. C.; Winkler, J. R.; Gray, H. B. *Chem. Biol.* **1996**, *3*, 491−497.
(11) Shastry, M. C. R.; Sauder, J. M.; Roder, H. *Acc. Chem. Res.* **1998**, *31*, 717−725.
(12) Bai, Y.; Sosnick, T. R.; Mayne, L.; Englander, S. W. *Science* **1995**, *269*, 192−197.
(13) Yeh, S.-R.; Han, S.; Rousseau, D. L. *Acc. Chem. Res.* **1998**, *31*, 727−736.
(14) Chan, C. K.; Hu, Y.; Takahashi, S.; Rousseau, D. L.; Eaton, W. A.; Hofrichter, J. *Proc. Natl. Acad. Sci. U.S.A.* **1997**, *94*, 1779−1784.
(15) Hagen, S. J.; Eaton, W. A. *J. Mol. Biol.* **2000**, *301*, 1019−1027.
(16) The equine cyt *c* numbering system is used throughout the text.
(17) Colón, W.; Wakem, L. P.; Sherman, F.; Roder, H. *Biochemistry* **1997**, *36*, 12535−12541.
(18) Yeh, S.-R.; Takahashi, S.; Fan, B.; Rousseau, D. *Nature Struct. Biol.* **1997**, *4*, 51−56.
(19) Telford, J. R.; Tezcan, F. A.; Gray, H. B.; Winkler, J. R. *Biochemistry* **1999**, *38*, 1944−1949.

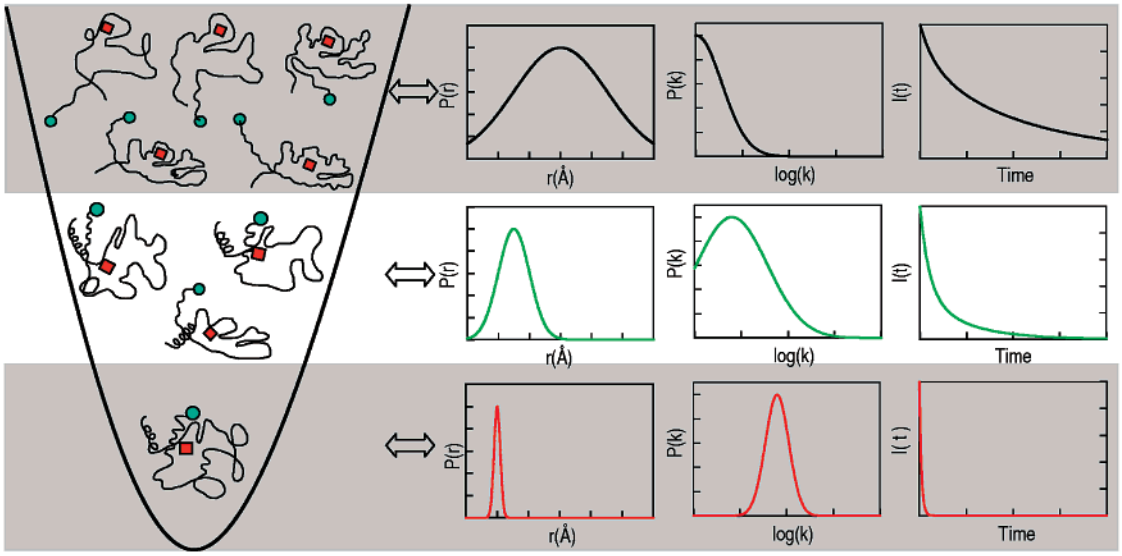

Figure 1. Schematic representation of the relationship between polypeptide conformations and fluorescence decay kinetics. An ensemble of unfolded proteins found near the top of a funnel-shaped landscape will have a broad distribution of distances ($P(r)$) between fluorescence energy transfer donors and acceptors. The distance distribution function can be transformed using eq 2 to a distribution over fluorescence decay rates (k), producing (eq 1) a slowly decaying fluorescence intensity profile ($I(t)$). An ensemble of folded proteins (bottom of the funnel) will have a narrow distance distribution, and faster excited-state decay.

with a dansyl fluorophore (DNS); the DNS label fluoresces intensely when the protein is unfolded in guanidine hydrochloride (GuHCl) solutions, but is significantly quenched by energy transfer to the heme in the folded conformation.[20]

Experimental Section

Protein Derivatization: DNS(C102)-cyt *c*. The C102 sulfhydryl group of *S. cerevisiae* iso-1 cytochrome *c* (Sigma) was derivatized with the thiol-reactive fluorophore 5-(((((2-iodoacetyl)amino)ethyl)amino)-naphthalene-1-sulfonic acid (1,5-I-AEDANS, Molecular Probes). Fe(III)cyt *c* (50 mg) was dissolved in degassed sodium phosphate buffer (NaP_i, 2 mL, pH 7.3, μ 0.1 M) and urea (1 g) was added to denature the protein. Dropwise addition of a 3-fold molar excess of 1,5-I-AEDANS in water (5 mg/300 mL) proceeded over a 1.5 h time period. After 2.5 h, the reaction was quenched by the addition of dithiothreitol (DTT, ICN Biomedical, Inc.). The derivatization reaction was performed in the dark to minimize deleterious photochemical side reactions. Protein was separated from 1,5-I-AEDANS and DTT by gel filtration chromatography (Sephadex G-25, Sigma, bead size 20−80 mm, 5 mL/g dry gel, swollen in H_2O, eluted with NaP_i, pH 7, μ 0.1 M) and further purified by ion-exchange chromatography (Pharmacia FPLC, Mono S column).

Model Compound Synthesis. The *N*-acetylcysteine derivative of AEDANS was prepared according to a published procedure,[21] with minor modifications. 1,5-I-AEDANS (100 mg) was mixed with a ~10-fold molar excess of *N*-acetylcysteine (420 mg, Sigma) in 4 mL of NaP_i (pH 7, μ 0.1 M) for ~1 h. The solution pH was adjusted to ~7.0 with NaOH (1 M) and maintained at this level for an additional 1−2 h. The solution pH was then adjusted to 2.0 with concentrated HCl and the mixture was cooled to 4 °C. After ~24 h, a small amount of precipitate had formed, and the solution was rotovaped to dryness. The residue was washed with ether and recrystallized from hot water. The recrystallized material was washed with at least 300 mL of acetone to remove excess *N*-acetylcysteine and again recrystallized from hot water. The resulting pale yellow-green prismatic crystals were air-dried at room temperature.

Fluorescence Decay Kinetics. Fluorescence decay measurements were performed using the third harmonic of a regeneratively amplified, mode-locked Nd:YAG laser (355 nm, 50 ps, 0.5 mJ) for excitation, and a picosecond streak camera (Hamamatsu C5680) for detection. Magic-angle excitation and collection conditions were employed throughout. DNS fluorescence was selected with a long-pass cutoff filter (>430 nm). The C5680 was used in the photon-counting mode for luminescence-decay measurements on samples at equilibrium; the analogue mode was employed for measurements on transient species.

Equilibrium Unfolding. DNS(C102)-cyt *c* was denatured by high concentrations of guanidine hydrochloride (GuHCl, Sigma). The extent of unfolding was monitored by absorption and circular dichroism (CD) as well as by measurements of DNS fluorescence intensity and decay kinetics.

Refolding Kinetics. Protein folding was initiated by using a BioLogic SFM-4s stopped-flow mixer. The calculated mixing deadtime was ~1.1 ms. To test the mixing efficiency, we added $[Ru(bpy)_3]Cl_2 \cdot 6H_2O$ (bpy = 2,2′-bipyridine, Strem, 1 mM) to the GuHCl syringe and $[Ru(NH_3)_6]Cl_3$ (Strem, 56 mM) to the buffer syringe. Luminescence decay measurements revealed uniform quenching of excited $Ru(bpy)_3^{2+}$ by $Ru(NH_3)_6^{3+}$ immediately (1 ms) after stopped-flow dilution, confirming that the solutions from the two syringes were completely mixed.

FET kinetics were measured during DNS(C102)-cyt *c* folding by synchronizing the picosecond Nd:YAG laser with the stopped-flow mixer and streak camera. A gate and delay generator (Stanford Research Systems, Model DG535) was used to program variable delay times between mixing and laser excitation of DNS. Data from 10 to 20 laser shots ([DNS(C102)-cyt *c*] 10 μM; 200 μL per stopped flow mixing cycle; one laser shot per mix) provided adequate signal-to-noise levels. For cyt *c* refolding kinetics experiments performed in the presence of imidazole (150 mM, Sigma), both the guanidine and the diluting buffer syringes contained the added heterocycle.

Data Analysis. To extract distributions of **D**−**A** distances from the luminescence decay kinetics, we must first obtain $P(k)$ by inverting the discrete Laplace transform that describes $I(t)$ (eq 1).

$$I(t) = \sum_{k=k_0}^{\infty} P(k) \exp(-kt) \qquad (1)$$

(20) Telford, J. R.; Wittung-Stafshede, P.; Gray, H. B.; Winkler, J. R. *Acc. Chem. Res.* **1998**, *31*, 755−763.
(21) Hudson, E. N.; Weber, G. *Biochemistry* **1973**, *12*, 4154−4161.

Transformation to a probability distribution over r ($P(r)$) is readily accomplished using eq 2.[22] The value of k_o (9.6×10^7 s^{-1}) was obtained from luminescence

$$k = k_o + k_o\left(\frac{r_o}{r}\right)^6 \qquad (2)$$

decay measurements with the DNS-cysteine model complex.

The difficulty in obtaining $P(r)$ arises in the first step because numerical inversion of $I(t)$ is extremely sensitive to noise.[23] Regularization methods that impose additional constraints on the properties of $P(k)$ have been developed to stabilize inversion problems of this type. The simplest constraint that applies to the FET kinetics data is that $P(k) \geq 0$ ($\forall k$). Data were fit using a MATLAB (The Math Works, Inc.) algorithm (LSQNONNEG) that minimized the sum of the squared deviations (χ^2) between observed and calculated values of $I(t)$, subject to a nonnegativity constraint. LSQNONNEG fitting produced narrow $P(k)$ distributions with relatively few nonzero components. Information theory suggests that the least biased solution to this inversion problem minimizes χ^2 *and* maximizes the breadth of $P(k)$.[23] This regularization condition can be met by maximizing the Shannon−Jaynes entropy of the rate-constant distribution ($S = -\sum_k P(k)\ \ln\{P(k)\}$), implicitly requiring that $P(k) \geq 0$ ($\forall k$).[24] Maximum entropy (ME) fitting produced stable and reproducible numerical inversions of eq 1. The balance between χ^2 minimization and entropy maximization was determined by graphical L-curve analysis.[25] The $P(k)$ distributions from ME fitting were broader than those obtained with LSQNNONEG fitting, but exhibited comparable maxima. The results from LSQNONNEG fitting are given in the Supporting Information. A simple coordinate transformation defined by eq 2 was used to recast the $P(k)$ results obtained from ME and LSQNONNEG fitting as probability distributions over r.

Results

Equilibrium Unfolding. The rate of energy transfer is equal to the decay rate of the unquenched fluorophore (k_o) when the **D**−**A** distance is equal to the critical length (r_o).[22] Under typical conditions, FET rates can be measured for **D**−**A** distances in the range $0.3r_o \leq r \leq 1.5r_o$. The critical length ($r_o$) of the DNS-heme FET pair is 40 Å, meaning that a 12−60 Å **D**−**A** distance range can be probed in the modified protein. In the folded protein, DNS FET kinetics transform into a distribution function with a mean **D**−**A** distance of 25 Å and a full-width at half-maximum (fwhm) of ∼5 Å (Supporting Information, Figure S1). Addition of GuHCl (<0.5 M) leads to an increase in DNS fluorescence, owing to an increase in the breadth of the distribution centered at 25 Å, along with the appearance of a small population of polypeptide with $\bar{r} > 50$ Å. As [GuHCl] increases above 0.5 M, the small-r distribution loses amplitude as it broadens and moves to a slightly larger mean value (∼29 Å), and there is a concomitant increase in the amplitude of the $\bar{r} > 50$ Å population.[26] Finally, at high [GuHCl] (>1.2 M), most of the protein is in an extended conformation ($r > 40$ Å), although a small fraction (∼10%) retains a more compact structure with $\bar{r} \sim 29$ Å. Addition of imidazole at high denaturant concentrations has no effect on this compact species. The GuHCl-induced variations in the distribution of **D**−**A** distances are consistent with cooperative unfolding of DNS-(C102)-cyt *c*, but the FET kinetics reveal structural features that are not apparent from steady-state spectroscopic measurements.

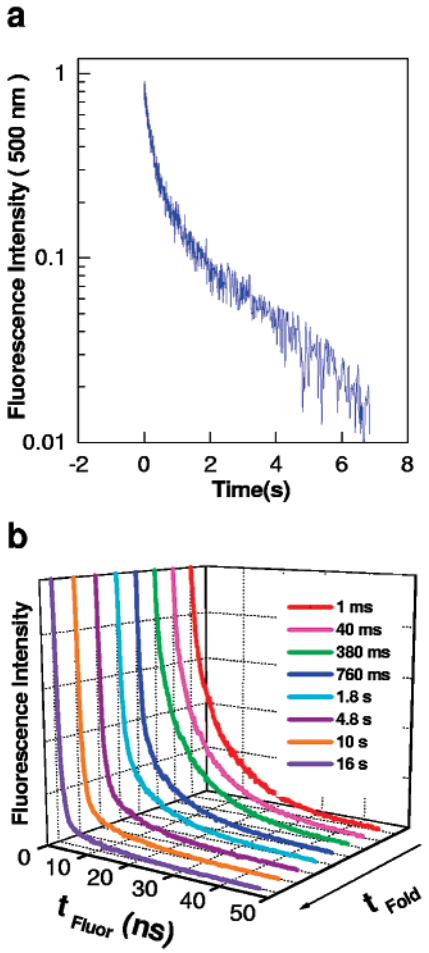

Figure 2. (a) Time dependence of DNS fluorescence (λ_{obsd} = 500 nm) intensity during DNS(C102)-cyt *c* refolding ([GuHCl] = 0.13 M, pH 7, 22 °C, λ_{ex} = 325 nm). (b) DNS fluorescence decay kinetics measured at the indicated times after initiation of DNS(C102)-cyt *c* refolding (λ_{obsd} > 430 nm; λ_{ex} = 355 nm).

Refolding Kinetics. The DNS fluorescence intensity, a measure of the ensemble-averaged extent of folding in DNS-(C102)-cyt *c*, exhibits a biphasic kinetics profile when the refolding is triggered by stopped-flow dilution of GuHCl (1.3 to 0.13 M, pH 7, 22 °C) (Figure 2a). The major fraction (90%) of the decrease in fluorescence occurs within 2 s of mixing; the remaining 10% of the signal change proceeds in the 2−10 s time interval. The integrated DNS fluorescence provides an indication of the extent of folding, but reveals nothing about the structural heterogeneity of the protein ensemble.

Measurements of $I(t)$ at various times during folding (Figure 2b) provide snapshots of **D**−**A** distance distributions, $P(r)$. Immediately after the folding is triggered (1 ms), we find that 40% of the protein ensemble has collapsed, producing a population with an average **D**−**A** distance of ∼27 Å (Figure 3). Surprisingly, 60% of the protein remains in extended conformations with **D**−**A** distances greater than 40 Å. Within 10 ms, the $P(r)$ distribution develops a component at $\bar{r} = 25$ Å, a value comparable to that of the folded protein. By 50 ms, the 25-Å component is larger than the 27-Å population, and after 400 ms, the latter fraction has nearly disappeared. Concomitant

(22) Förster, T. *Ann. Phys.* (*Leipzig*) **1948**, *2*, 55−75.
(23) Istratov, A. D.; Vyvenko, O. F. *Rev. Sci. Instrum.* **1999**, *70*, 1233−1257.
(24) Livesey, A. K.; Brochon, J. C. *Biophys. J.* **1987**, *52*, 693−706.
(25) Lawson, C. L.; Hanson, R. J. *Solving Least Squares Problems*; Prentice Hall: Englewood Cliffs, NJ, 1974.
(26) The 40 Å critical length limits the **D**−**A** distances that can be measured in unfolded DNS(C102)-cyt *c*, and prevents us from obtaining accurate distributions at large r values. Consequently, the single bars at 53 Å in the distributions represent the populations of peptides with $r \geq 53$ Å.

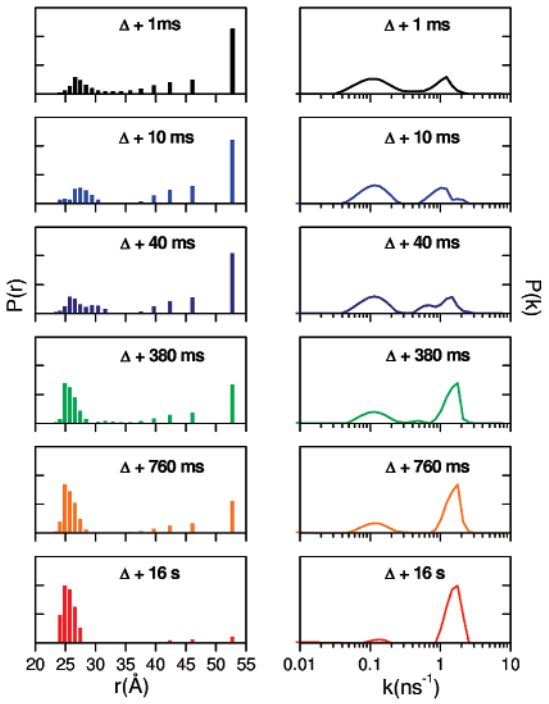

Figure 3. Evolution of the distributions of luminescence decay rates ($P(k)$, right) and **D**−**A** distances ($P(r)$, left) during the refolding of DNS(C102)-cyt *c* ([GuHCl] = 0.13 M, pH 7, 22 °C; Δ is the mixing deadtime).

with the evolution of the collapsed ensemble, there is a decrease in the population of extended conformations.

The formation of correctly folded cyt *c* at pH 7 is limited by heme axial ligand substitution processes.[18] Displacement of misligated His groups in denatured cyt *c* by imidazole ([imidazole] = 0.15−0.25 M, pH 7) dramatically accelerates refolding.[27] NMR investigations of the imidazole adduct of equine cytochrome *c* reveal only modest disruption of the protein structure in the vicinity of the M80 residue.[28] Measurements of FET kinetics during DNS(C102)-cyt *c* refolding in the presence of imidazole (0.15 M) at room temperature indicate that the native **D**−**A** distance distribution is formed in less than 20 ms. At lower temperature (1 °C), the evolution of **D**−**A** distance distributions (Supporting Information, Figure S4) is remarkably similar to that in the absence of imidazole. The key difference is the overall time scale of refolding; formation of folded protein is largely complete within 200 ms. Roughly equal populations of extended ($\bar{r}$ > 50 Å) and collapsed ($\bar{r}$ = 32 Å) structures are observed immediately after folding is triggered. The 32-Å distribution evolves into a 25-Å native distribution in ∼200 ms.

Discussion

The FET kinetics measured during DNS(C102)-cyt *c* folding indicate that dilution of denaturant to concentrations favoring native protein conformations ([GuHCl] = 0.13 M) does not produce a complete collapse of the polypeptide ensemble. Within the deadtime of stopped-flow measurements, we find that only half of the protein population has formed compact structures. The compact ensemble (**C**) is characterized by a mean DNS−heme separation of ∼27 Å. This distance is greater than that of the native protein, indicating that the collapsed species

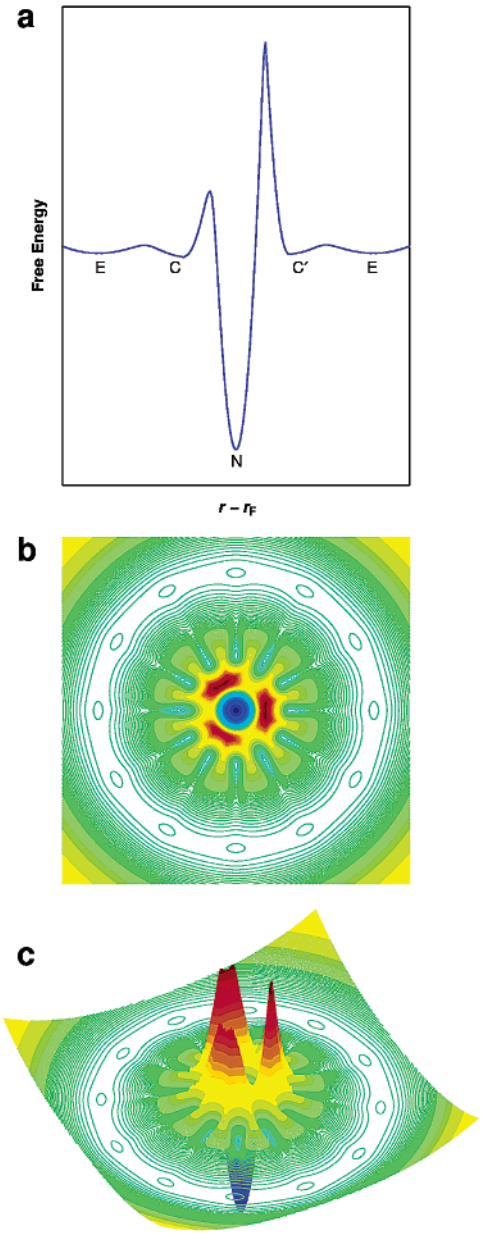

Figure 4. Idealized representations of the DNS(C102)-cyt *c* folding landscape. The lateral dimension in all plots is the deviation from the native **D**−**A** distance (∼25 Å). The two-dimensional cross-section of the landscape (a) shows nearly degenerate, shallow energy minima corresponding to extended (**E**) and collapsed (**C**, **C**′) conformations. The collapsed structures on the left side (**C**) of the global energy minimum can surmount a ligand substitution barrier (which can be lowered by the addition of imidazole) to reach the native (**N**) structure. Collapsed peptides on the right side (**C**′) face a high barrier to formation of the native fold; this population must exchange with other collapsed structures with lower barriers to folding. A contour plot (b) and three-dimensional representation (c) of this idealized folding landscape for DNS(C102)-cyt *c* reveal a flat region on the periphery for extended and compact polypeptides that surrounds the global energy minimum. Some of the compact structures are separated from the native fold by low energy barriers. The remainder have high barriers to native state formation. Polypeptides that fall into these minima must rearrange to extended conformations that can collapse into productive compact structures.

are not fully folded.[29] As the population of proteins with the native fold (**N**) increases, the extended (**E**) and compact populations disappear on comparable time scales.

It is surprising that such a large fraction of the protein ensemble remains in an extended conformation after denaturant dilution. These extended conformations are not a consequence

(27) Elöve, G.; Bhuyan, A. K.; Roder, H. *Biochemistry* **1994**, *33*, 6925−6935.
(28) Banci, L.; Bertini, I.; Liu, G.; Lu, J.; Reddig, T.; Tang, W.; Wu, Y.; Yao, Y.; Zhu, D. *JBIC* **2001**, *6*, 628−637.

of His misligation in the unfolded protein; high concentrations of imidazole displace the His ligands and speed refolding, yet both **E** and **C** fractions are observed at 1 °C. The accelerated cyt *c* refolding in the presence of imidazole also demonstrates that **E** does not arise from kinetically trapped conformations containing proline isomers or incorrect topomers; there is no obvious mechanism by which 150 mM imidazole could eliminate such traps. Indeed, the parallel disappearance of **E** and **C**, rapidly in the presence of imidazole, slowly when His residues misligate the heme, strongly suggests that the two populations are in rapid equilibrium.[30]

The time-resolved **D**−**A** distance distributions extracted from FET measurements lead to an *idealized* folding landscape for DNS(C102)-cyt *c* (Figure 4). The lateral dimension of the landscape is the deviation of the **D**−**A** distance from its value in the folded protein ($r - r_F$; $r_F \sim 25$ Å); and the vertical axis reflects the polypeptide free energy. The cross-section of this landscape (Figure 4a) illustrates two possible fates for a polypeptide that was in an extended conformation ($r > 40$ Å) prior to the initiation of folding. Denaturant dilution shifts the **E** ⇌ **C** equilibrium to produce comparable populations of extended and compact polypeptides undergoing rapid exchange (∼100 μs). Collapsed conformations (**C**) with favorable arrangements of the polypeptide backbone (topologies) can transform into the native structure (**N**) at pH 7 by surmounting an energy barrier corresponding to a heme axial-ligand substitution process (Figure 4a, left path). Rapid collapse of a polypeptide is likely to produce conformations (**C′**) that cannot evolve into the native fold because of backbone-crossing barriers (topological frustration,[31] Figure 4a, right path). This model implies that the population of collapsed polypeptides is heterogeneous and that only a fraction of the collapsed conformers are competent to transform into **N**.[31,32]

For topologically frustrated compact conformations, the only route to the native state involves formation of an extended polypeptide that can recollapse to a more favorable structure. This mechanism is illustrated by two- and three-dimensional contour plots of the DNS(C102)-cyt *c* folding landscape (Figure 4b,c). The native fold is represented by the central free-energy minimum. Owing to the near degeneracy of collapsed and extended polypeptides, the landscape consists of a relatively flat outer rim surrounding a narrow funnel. Rapid interchange among extended conformations via intrachain diffusion proceeds on the outer rim of the landscape.[33−35] These extended polypeptides frequently fall into collapsed conformations toward the interior of the landscape; some of these (3 of the 12 collapsed conformers shown on the idealized surface) can form the native structure; the others must extend and try again. Collapsed and extended polypeptides in rapid equilibrium at the top of the funnel must wait for a ligand substitution event (pH 7) to open the way to conversion to the native structure at the bottom. Addition of imidazole lowers the ligand substitution barrier and speeds the transformation of collapsed polypeptides into the native form.

Conclusions

The picture that emerges is one in which extended polypeptide conformations play a pivotal role in DNS(C102)-cyt *c* refolding. Time-resolved FET measurements reveal that, at the onset of folding, fully half of the polypeptide ensemble is found in extended conformations reminiscent of the denatured protein.[36] *The near degeneracy and rapid equilibration of collapsed and extended populations would enable DNS(C102)-cyt c to escape from topologically frustrated compact structures that cannot produce the native fold because of extremely high energy barriers*.[31] If collapsed intermediates were substantially more stable than extended geometries, formation of extended structures would occur infrequently, exacerbating the problem of topological frustration.[31] Instead, DNS(C102)-cyt *c* can collapse and extend many times as it searches for compact structures that have low-barrier routes to the native conformation.[32]

Since collapsed cyt *c* intermediates are not considerably more stable than the fully denatured protein, the likelihood of a native structure rearranging to a partially folded species is substantially lower than would have been the case if collapsed conformations were found in deeper wells on the folding landscape. If this is a common protein folding characteristic, it may be an important means of avoiding the partially folded intermediates that can aggregate into the misfolded structures that characterize a variety of disease states.

Acknowledgment. We thank Jason Telford, Michael Machczynski, and I-Jy Chang for assistance during the initial stages of this project. This work was supported by the NSF (MCB-9974477, DBI-9876443), an NIH training grant and NSF graduate fellowship (J.G.L.), and the Arnold and Mabel Beckman Foundation.

Supporting Information Available: Plots of luminescence decay rates (PDF). This material is available free of charge via the Internet at http://pubs.acs.org.

JA017399R

(29) The mean fluorescence decay rate in the compact intermediate is ∼1.8 times faster than the decay rate in the folded protein. This small difference in decay rates is found regardless of the fitting method employed (biexponential, LSQNONNEG, ME). Adequate fits to the data cannot be obtained if the decay rate for the compact species is fixed equal to the decay rate for the folded protein. Furthermore, stopped-flow transient absorption measurements on equine cyt *c* demonstrate that M80 coordination to Fe at neutral pH requires several hundred milliseconds (Sosnick, T. R.; Mayne, L.; Hiller, R.; Englander, S. W. *Nature Struct. Biol*. **1994**, *1*, 149−156). It is unlikely, therefore, that the compact structures observed a few milliseconds after denaturant dilution are fully folded.

(30) A ∼100 μs time scale for **E** ⇌ **C** equilibration can be inferred from ultrarapid mixing studies of equine cyt *c* refolding probed by integrated W59 fluorescence.[11,15]

(31) Thirumalai, D.; Klimov, D. K.; Woodson, S. A. *Theor. Chem. Acc*. **1997**, *96*, 14−22.

(32) Debe, D., A.; Carlson, M. J.; Goddard, W. A., III *Proc. Natl. Acad. Sci. U.S.A.* **1999**, *96*, 2596−2601.

(33) Hagen, S. J.; Hofrichter, J.; Szabo, A.; Eaton, W. A. *Proc. Natl. Acad. Sci. U.S.A.* **1996**, *93*, 11615−11617.

(34) Hagen, S. J.; Hofrichter, J.; Eaton, W. A. *J. Phys. Chem. B* **1997**, *101*, 2352−2365.

(35) Lapidus, L. J.; Eaton, W. A.; Hofrichter, J. *Proc. Natl. Acad. Sci. U.S.A.* **2000**, *97*, 7220−7225.

(36) Time-resolved CD (Akiyama, S.; Takahashi, S.; Ishimori, K.; Morishima, I. *Nature Struct. Biol*. **2000**, *7*, 514−520) and small-angle X-ray scattering (Akiyama, S.; Takahashi, S.; Kimura, T.; Ishimori, K.; Morishima, I.; Nishikawa, Y.; Fujisawa, T. *Proc. Natl. Acad. Sci. U.S.A.* ***2002***, *99*, 1329−1334) measurements indicate that, after a few milliseconds of folding, the cyt *c* ensemble has partial helicity and a bimodal pair distribution function. These observations are fully consistent with the bimodal distribution of compact and extended conformations that we observed using time-resolved FET measurements.